

Sensitivity of Road Unevenness Indicators to Distresses of Composite Pavements

Peter MÚČKA¹

Abstract: The paper examined the sensitivity of nineteen road unevenness indicators (RUI) to the distresses (reflection cracks, transverse cracks) of the composite pavements. The simulated longitudinal road profiles with superimposed distresses were compared with the pure random part of profiles to estimate the difference in roughness. The influence of distress width, depth, density, and road data pre-processing (moving average base length and sampling interval) was estimated. Analysis of variance was provided to detect the significance of differences in estimated RUIs for distressed and random profiles. The most sensitive indicators to the presence of the reflection cracks were the root mean square (RMS) value in the short wave band, the road elevation spectrum parameters in the whole and short wave bands. A weak sensitivity was observed for the International Roughness Index (IRI), Ride Number (RN), Profilograph Index (PrI) or the road elevation RMS values in the long and medium wave bands.

DOI: 10.6135/ijprt.org.tw/2015.8(2).72

Key words: Composite pavement; Distress; International Roughness Index; Longitudinal road profile; Power spectral density; Straightedge.

Introduction

Pavements can be generally classified into two broad categories: (a) Flexible pavements and (b) Rigid pavements. The Federal Highway Administration (FHWA) also identifies a third type of pavement, called a composite pavement. Composite pavements are a combination of Hot Mix Asphalt (HMA) and Portland cement concrete (PCC) pavements. Occasionally, they are initially constructed as composite pavements, but more frequently they are the result of pavement rehabilitation (e.g., HMA overlay of PCC pavement). This type of rehabilitation action is used to restore the functional performance of an existing pavement and/or to increase the structural capacity in order to handle additional and heavier traffic.

Flexible pavements comprise 83.2 % of rural and urban roads in the USA, rigid pavements 6.9 %, and composite pavements 9.9 %. For rural roads, composite pavements comprise 19.7 % of interstate roads, 19.2 % of freeways and expressways, 15.5 % of other principal arterial, 13.5 % of minor arterial, and 4.2 % of major collectors. For urban roads, composite pavements comprise 28.6 % of interstate roads, 21.1 % of freeways and expressways, 21.9 % of other principal arterial, 12.1 % of minor arterial, and 5.4 % of major collectors [1].

Composite pavements are usually used to rehabilitate existing roadways rather than in new construction. Asphalt overlays are sometimes laid over distressed concrete to restore a smooth wearing surface. A disadvantage of this method is that the movement in the joints between the underlying concrete slabs usually causes cracks (called reflective cracks) in the asphalt. This is affected by thermal

expansion and contraction or deflection of the concrete slabs from truck axle loads.

A composite pavement structure, throughout its service life, may develop different types of distresses. The distresses that affect composite pavements are very similar to those of flexible pavements because of the exposure that the asphalt concrete layer has in the composite structure. The distresses may be grouped into three major categories: fracture (cracking), distortion, and disintegration [2]. A major distress type in composite pavements is reflection cracking or joint reflection cracking. The reflective cracks occur in the asphalt surface course of the composite pavement and that coincide with cracks with appreciable width or joints in the underlying layer. The cracks occur directly over the underlying cracks or joints. They are caused by the relative horizontal and vertical movement of these cracks or joints caused by temperature cycles and/or traffic loading. Hein *et al.* [3] referred that there is early (3 to 5 years) deterioration due to reflective cracking on the HMA from the underlying rigid layer's discontinuities in composite pavements.

The joint deteriorations such as spalling, breaking, cracking, chipping, or fraying of the slab edges usually occur within 50 mm of joints [4]. Reflection cracking presents cracks in a flexible overlay of PCC pavements that occur over the underlying cracks or joints [2, 5]. According to the severity level, this distress type is divided into three groups – low (mean width ≤ 6 mm), moderate (mean width > 6 mm and ≤ 19 mm), and high (mean width > 19 mm) [6]. Another classification of reflective cracks uses two groups: the low severity cracks (< 12.5 mm (1/2 inch) wide and infrequent cracks) and the high severity cracks (> 12.5 mm (1/2 inch) wide and numerous cracks).

The typical joint depth can reach several millimeters or several centimeters. An expansion joint width typically ranges from 1.5 to 2.5 cm and transverse contraction joints from 1 to 2 cm [7]. Most of the jointed PCC pavements have a joint spacing between 4.6 and 6.1 m (15 and 20 ft) [8, 9].

A sensitivity of nineteen road unevenness indicators (RUI) to the

¹ Institute of Materials and Machine Mechanics, Slovak Academy of Sciences, Račianska 75, 831 02 Bratislava 3, Slovakia.

⁺ Corresponding Author: E-mail ummsmuc@savba.sk
Note: Submitted April 29, 2014; Revised December 9, 2014; Accepted December 15, 2014.

road distresses of composite pavements was analyzed in this study. This is important, because various roughness indexes are intended for pavement rehabilitation consideration in Pavement Management System (PMS) as an overall serviceability condition of pavement sections and distress presence should distort the final values of particular RUIs.

The contemporary research in this field is predominantly focused on the PCC pavements and quantification of the influence of the vertical faults, i.e., vertical shifts between adjacent slabs, on ride quality (Khazanovich *et al.* [10], Perera and Kohn [11], Selezneva *et al.* [12], Byrum and Perera [13] and Liu and Wang [14]). The influence of joint width, joint depth, joints spacing, or the road data processing was examined by Byrum [8], Wen and Chen [9], Morian *et al.* [15] and Hall and Crovetto [16].

The influence of the joints on ride quality is often quantified with the IRI statistics. The published results do not allow to distinguish between the contribution of the random profile part and the distress part to the final value of roughness index.

The main objectives of this study are as follows:

- To create an algorithm and program code for generation of the artificial longitudinal road section with superimposed reflection cracks with controlled dimensions and for the estimation and mutual comparison of the commonly used road unevenness indicators (RUI);
- To study the influence of particular crack dimensions – crack depth, crack width, distance of successive cracks on the RUIs;
- To compare the RUI values calculated for the pure random profile with those calculated for the raw profile with distresses;
- Apply the analysis of variation on the results to detect a significance of differences for particular RUIs;
- To examine the influence of road data pre-processing on the results.

Overview of the Road Unevenness Indexes and Devices

US states Department of Transportation (DOT) practices related to the roughness measurement use the different road unevenness indexes (Table 1) according to the type of wearing courses (PCC vs. Asphalt concrete (AC)) [17]. Table 1 shows the number of US states from total number of fifty US states that use the particular roughness index. Profilograph Index (~ 60 % of US states) and IRI (~ 30 %) are the most frequently used indices. Profilograph (55 % for PCC surfaces and 26 % for AC surfaces) and Inertial Profilometer (~ 40 % for PCC surfaces and 68 % for AC surfaces) are the most frequently used measurement devices. The following roughness indexes are currently used in the United States: IRI, Mean Roughness Index (MRI), Half-car Roughness Index (HRI), PrI, RN, Mays Ride Number (MRN), Cumulative Straightedge Index (CSI), and Ride Quality Index (RQI) [17].

The IRI, straightedge parameters, road elevation power spectral density (PSD) parameters and the three-wave band indicators are frequently used for road unevenness characterization in Europe (Willet *et al.* [18], Boscaino and Praticò [19], Delanne and Pereira

Table 1. The Number of US States that Use the Particular Road Roughness Indexes.

Road Surface Type	PCC	HMA
Profilograph Index	28	31
IRI	15	14
Ride Number	—	2
Other	3	3

[20] and Praticò [21]). The inventory of road unevenness measuring devices was provided by Boscaino and Praticò [19].

The Road Unevenness Indicators

The review of commonly used indicators of longitudinal unevenness of roads and airfield runways was provided by Willet *et al.* [18], Boscaino and Praticò [19], Praticò [21], Sayers and Karamihas [22], Wilde [23], Chemistruck *et al.* [24] or in Smoothness Specifications Online [17]. Several road unevenness indicators used in this study (IRI, PSD parameters, and three-wave band indicators) are included into the standard proposal prEN 13036-5 [25], which standardizes various possible characterizations of road profile unevenness.

The road elevation PSD parameters are besides road quality estimation important for the vehicle industry for the testing and modeling purposes. The raw spectrum or its suitable analytical approximation allows a simple generation of synthetic road signal. The simplest model of the road elevation PSD, $G_H(\Omega)$, is often applied in the form [25–27]

$$G_H(\Omega) = C \Omega^{-w} \quad (1)$$

where Ω (rad/m) is the angular spatial frequency, C (rad^{w-1} m^{3-w}) = $G_H(1)$ is the unevenness index, w is the waviness.

Eq. (1) represents a line on a log-log chart with C as the vertical ordinate at the reference angular frequency $\Omega_0 = 1$ rad/m and w as the slope of the line. C is proportional to the unevenness variance and w expresses the amplitude distribution between particular spatial frequency bands.

The road elevation PSD parameters C and w [Eq. (1)] were evaluated based on processing defined in the ISO 8608. The ISO 8608 defines the fitting interval of the raw PSD by a straight line in the angular spatial frequency range, $\Omega = 0.069–17.77$ rad/m, i.e., in the wavelength range, $L = 0.35–90.9$ m.

Two-band indicators were obtained by fitting a raw PSD by two straight-lines in a range, 0.35–90.9 m. Values C_L and w_L are given for the long-wave band ($\Omega < 1$ rad/m), and C_S and w_S for the short-wave band ($\Omega > 1$ rad/m). Unevenness indexes, C_L and C_S , are valid for $\Omega = 1$ rad/m. Andrén [26], Kropáč and Múčka [28] and Múčka [29] provided that two lines approximation of PSD better fits the raw road spectrum. The PSD parameters are explained in Fig. 1 with fitting of a raw spectrum of real composite profile (Section #180606) in one and two wave bands.

Three-band indicator system is used in some European countries [20]. Three-band indicators define the road profile in the three wave bands: short waves, 0.78125 to 3.125 m ($\Omega = 2.01–8.04$ rad/m); medium waves, 3.125 to 12.5 m ($\Omega = 0.5–2.01$ rad/m), and long waves, 12.5 to 50 m ($\Omega = 0.126–0.5$ rad/m). The RMS values of the

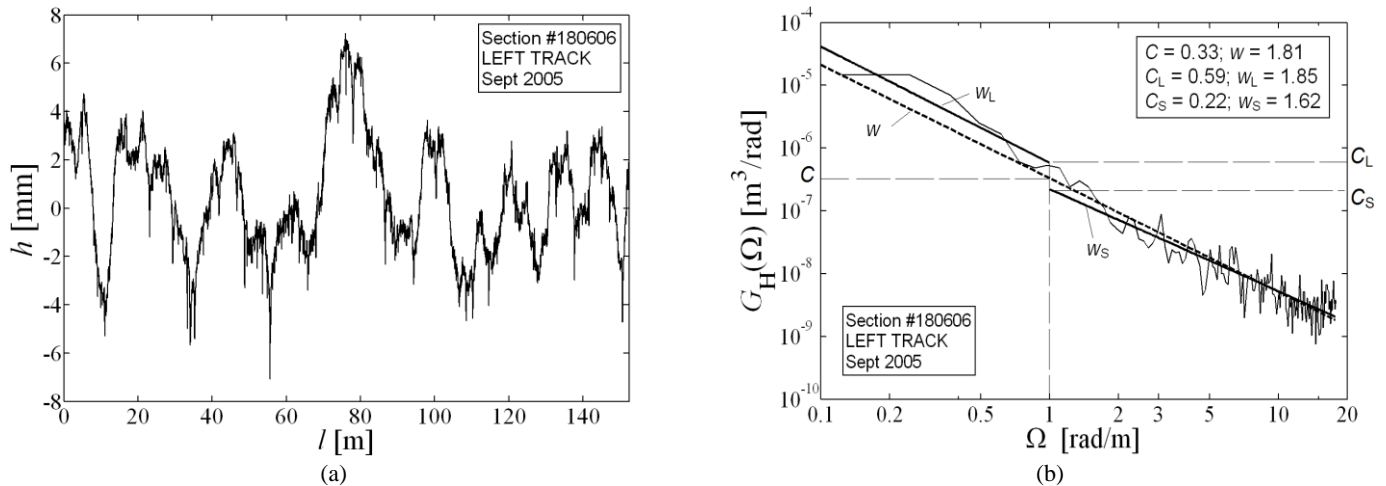


Fig. 1. Section #180606 (Left Track) Measured in September 2005: (a) Road Elevation, (b) Road Elevation Power Spectral Density.

longitudinal road profile elevation in the long- (RMS_L), medium- (RMS_M), and short (RMS_S) wave bands are recognized in the prEN 13 036-5 [25] as the possible indicators of road unevenness.

The IRI index uses a computer-based virtual response-type system based on the response of a reference quarter-car vehicle model as it traverses a tested pavement section at a constant speed of 80 km/h. The IRI is defined as the integral of absolute difference in suspension vertical velocity between axle and sprung mass of the quarter car model with respect to road section length with units of slope mm/m or in/mi. The algorithm was proposed by Sayers [30] and is also implemented in the prEN 13036-5 [25] or in the American Society for Testing and Materials (ASTM) Standard E1926-98 [31]. The IRI statistics is often used in the PMS and in the transportation/highway engineering community.

The Ride Number is based on the mathematical processing of the longitudinal profile to produce an estimate of subjective ride quality [32]. The ride number analysis method shares features with the IRI and uses the same filtering method. The filtered profile is reduced to yield a RMS value called Profile Index (PI) that has units of dimensionless slope. RN is defined as an exponential transform of PI according to the equation, $RN = 5e^{-160PI}$.

Variance of the road elevation was obtained by integration of the road elevation PSD in the wave band from 0.35 m to 90.9 m. The road elevation RMS value, RMS_H , is a square root of variance D_H . RMS_H indicator is recommended in the ISO 8608 for general characterization of a road profile.

The Profilograph Index is a parameter based on the processing of a pavement profile trace, which is obtained by mechanized or computerized profilograph. The PrI estimation involves placing the blanking band of defined height and length over the profile trace, while the excursions are evenly distributed above or below the opaque blanking band. The deviations of profile trace above and below the blanking band are counted. The deviations should be of defined minimal vertical and horizontal dimensions. The sum of the recorded heights within a given segment will be the PrI for that segment. The deviation count is then derived by the section length. The PrI estimation procedure was described by Perera and Kohn [11], Song and Teubert [33], or Shon *et al.* [34]. The California Profilograph Index is defined in the ASTM E1274-03 Standard [35]. The California profilograph measures the vertical deviations from a

moving 7.62-m (25-foot) reference plane. The index is reported in inches per mile and uses a 5.08-mm (0.2-inch) blanking band. The approach for PrI estimation according to Song and Teubert [33] was used, which is implemented in ProFAA software. ProFAA is the Federal Aviation Administration's computer program for computing pavement elevation profile roughness indexes. The profilograph trace is low-pass filtered by 3rd order Butterworth filter and sampled by 2.5 cm.

The straightedge (SE) approach is based on the measurement of clearance between the road surface and a straightedge [22, 36, 37]. The straightedge approach is frequently used for the acceptance of individual pavement layers covered successively in the course of pavement construction.

Two types of straightedge were considered:

- (a) Physical straightedge: the physical straightedge rests on the two highest points of the pavement profile beneath the straightedge. The vertical distance from the straight line representing the straightedge to each of the profile sample points beneath the straightedge is computed. The maximum value of all the vertical distances is reported as the maximum deviation from the straightedge over its full length or between the straightedge supports.
- (b) Rolling straightedge: one end of the straightedge is set on a specified profile point and the other end of the straightedge is set on a corresponding profile sample point. These two points then define the straight line defining the simulated straightedge. The maximum deviation of the interior profile points from the straight line is found and reported as the maximum deviation. The other approach records a deviation in the middle of the straightedge, i.e., mid-cord deviation (MCD).

Five types of straightedge variables (Fig. 2) were evaluated:

- $2A_B$ (mm) – the maximum deviation between the supports;
- $2A_F$ (mm) – the maximum deviation over full straightedge length;
- $2A_{RSE}$ (mm) – the maximum deviation of the interior profile points from the straight line;
- MCD (mm) – the mid-cord deviation between the road profile and the rolling straightedge (reference line) in the middle of the rolling straightedge;

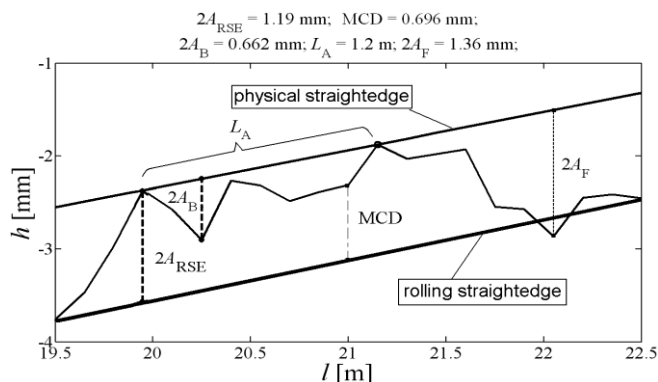


Fig. 2. Scheme of Various Straightedge Indexes Estimation for Physical and Rolling Straightedge.

- VA (mm/m^2) – vertical acceleration represents the second derivative of the road profile or the change of slope at a given point. The vertical acceleration is equivalent to the MCD. The vertical acceleration equals an MCD multiplied by $2/B^2$ ($B = \Lambda/2 =$ base length, $\Lambda =$ straightedge length).

Three types of straightedge variables ($2A_B$, $2A_F$, $2A_{RSE}$) were expressed as the mean values (denoted as $\langle \cdot \rangle$) per section length, and the MCD variable was expressed as the standard deviation (σ_{MCD}). An alternative to the MCD variable is RMSVA [22, 36, 37]. In this study, the straightedge length $\Lambda = 3$ m, with a shift of $\Lambda/2 = 1.5$ m was used.

Literature Survey

The various published reports and papers (Selezneva *et al.* [12], Liu and Wang [14], Morian *et al.* [15], Perera *et al.* [38]) were mainly oriented on the influence of the slab vertical faults, i.e., shift of the adjacent PCC slabs, on the IRI. The influence of the joint width, joint depth, joints spacing, or road data processing on the commonly used unevenness indexes was provided by Byrum [8], Wen and Chen [9], Morian *et al.* [15], and Hall and Croveti [16].

Morian *et al.* [15] analyzed the sections (SPS-4 database) from the Long-Term Pavement Performance (LTPP) Program and showed no differences in IRI between the sealed-joint and unsealed-joint sections. In Khazanovich *et al.* [10], a positive correlation between mean joint vertical faulting and IRI was reported. The spalled joints increase from 0 to 100 percent increased the IRI by 0.11 m/km. Perera *et al.* [38] reported the strong correlation between IRI and faulting for LTPP jointed plain concrete pavements (JPCP) sections [38]. Selzeneva *et al.* [12] identified the real dimensions of the joint vertical faults for doweled and un-doweled LTPP test sections. The obtained maximum values were about 5 mm for un-doweled sections and 3 mm for doweled sections. The increase in the IRI by 0.21 mm/m for 1 mm joint vertical fault was identified. It was shown, that joint spacing significantly affects the faulting. Hall and Croveti [16] analyzed the influence of the unsealed-joint and the sealed-joint sections on the IRI for the LTPP test sections. At three of the five sites, the rate of IRI increase was highest in the 3-mm unsealed group of sections. Byrum [8] quantified the effect that a slab curvature has on jointed concrete pavement IRI values. The curling or warping present in PCC slabs affects the IRI. The presence of curling or warping in the PCC slab caused the increase

in IRI. Byrum and Perera [13] presented three methods for comparing faulting to the IRI values for roadways. The faulting along the roadway has the gain of about 1.75 when converted to IRI, i.e., for each 1.58 m/km of faulting present, about 2.76 m/km of IRI will develop. Wen and Chen [9] indicated that joint spacing is not a statistically significant factor that affects the initial pavement roughness described by IRI. Liu and Wang [14] derived a linear relation between IRI and the joint vertical fault for the simulated profiles. The IRI increased by 0.3 mm/m per 1 mm of joint fault. The used joint width was 6.4 mm and the tire enveloping effect was involved into the analytical solution. Chang *et al.* [39, 40] created the software for automated fault measurement to detect faults and their parameters from the stored road test sections. The joint faults were identified without additional pre-filtering and with a sampling interval of 4 mm. Byrum [41] described a method for identifying and quantifying the fault size at each joint and crack. Múčka [42] analyzed the influence of the slab length on the conversion relationships between IRI and various straightedge indexes. The conversion relationships were practically unchanged for the slab length longer than 5 m.

The Road Profile Generator

The algorithm of the artificial road profiles generation, processing and RUIs evaluation is presented in Fig. 3. The random profile was generated based on the pre-defined PSD parameters; unevenness index, $C_{NOM} = 0.5$ rad m, and waviness, $w_{NOM} = 2.5$. These values were identified in Múčka and Kropáč [43] as the mean values of the pure random part of the various road surfaces (AC, PCC and composite) obtained by processing of 25,830 LTPP road records.

The length of the simulated profiles was $L = 150$ m, which is a typical length in the LTPP program. Ten random repetitions of the longitudinal profile were generated and processed. The distance between successive cracks was set, $l_D = 5$ m. The randomly chosen location of the first crack in the interval $(0, l_D)$ was considered. The crack depth and width were considered to be random numbers with uniform distribution.

Crack profile can be of various shapes – V-shape, U-shape, rectangular pulse, etc. For simplicity, cracks were modeled as the rectangular pulses. Saw and seal is an effective tool in eliminating maintenance costs associated with transverse reflective cracks. Saw cut applied to the reflective crack is of rectangular shape. Seal damage in particular crack can be approximately of a rectangular shape too.

The simulated profiles were digitalized with a sampling interval $\Delta l = 1$ mm to cover the true shape of the narrow cracks. Then the profiles were resampled with a sampling interval $\Delta l = 2.5$ cm.

Fig. 4 shows an example of the generated artificial profile with superimposed cracks. The influence of the road profile processing is shown in Fig. 5. The original profile with cracks (sampled by 1 mm) [Fig. 5(a)] was resampled to an interval of 2.5 cm [Fig. 5(b)] and then a 30-cm moving average and resampling to 15-cm was applied [Fig. 5(c)]. The distortion of the true crack shape caused by elevation data pre-processing is illustrated in Fig. 6. In Fig. 7, the crack main dimensions – crack depth, d_D , and crack width, w_D , are schematically depicted.

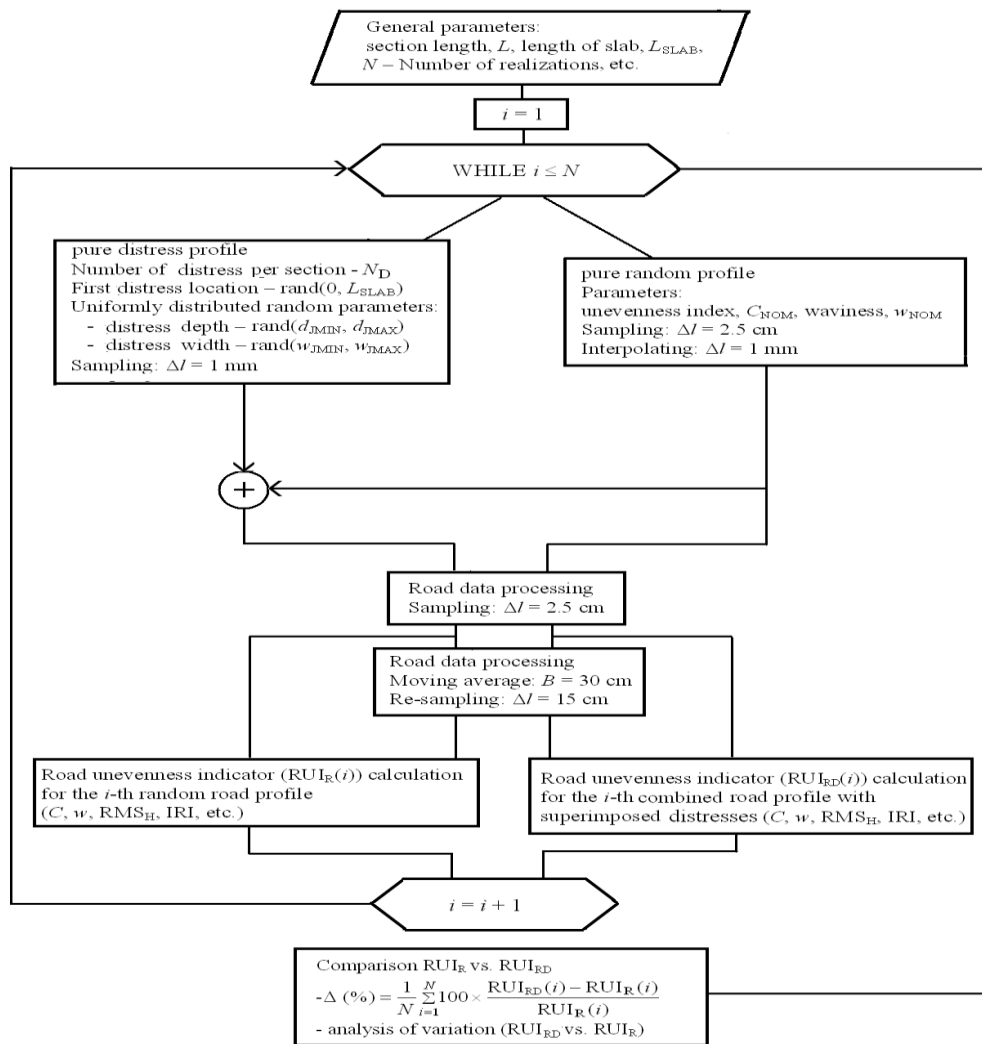


Fig. 3. Scheme of the Road Profile Generator with Comparison of the Road Quality for the Pure Random Profile versus Combined Random Profile with Distresses.

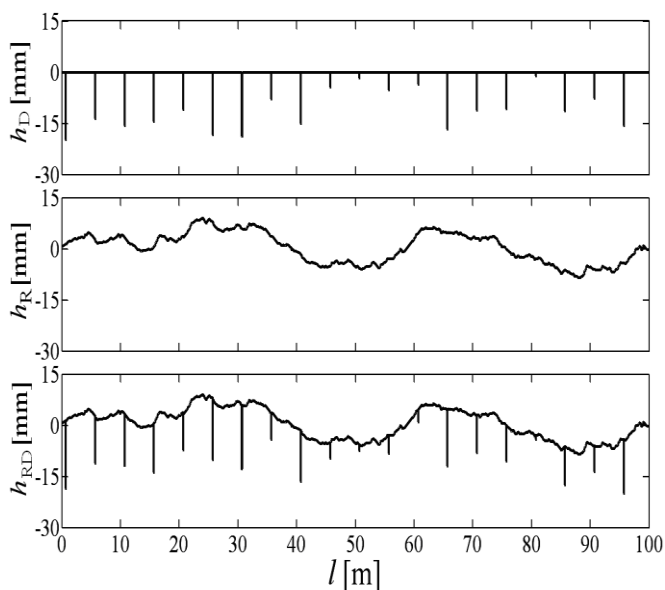


Fig. 4. Simulated Composite Road Profile: (a) The Pure Distress Part; (b) The Pure Random Profile; (c) The Random Road Profile with Superimposed Distresses.

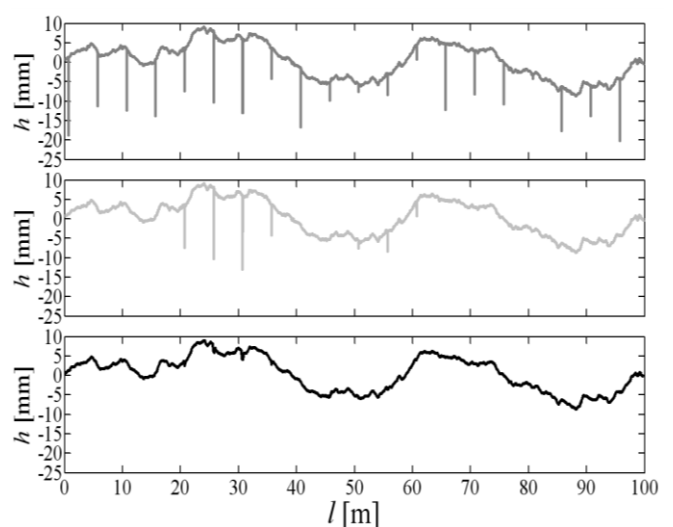


Fig. 5. The Influence of the Moving Average and Resampling on the Reflection Cracks Dimensions: (a) Simulated Road Profile with Superimposed Distresses, $\Delta l = 1$ mm, (b) Resampled Profile, $\Delta l = 2.5$ cm; (c) Moving Averaged Profile with Base Length, $B = 30$ cm, and Resampled to $\Delta l = 15$ cm.

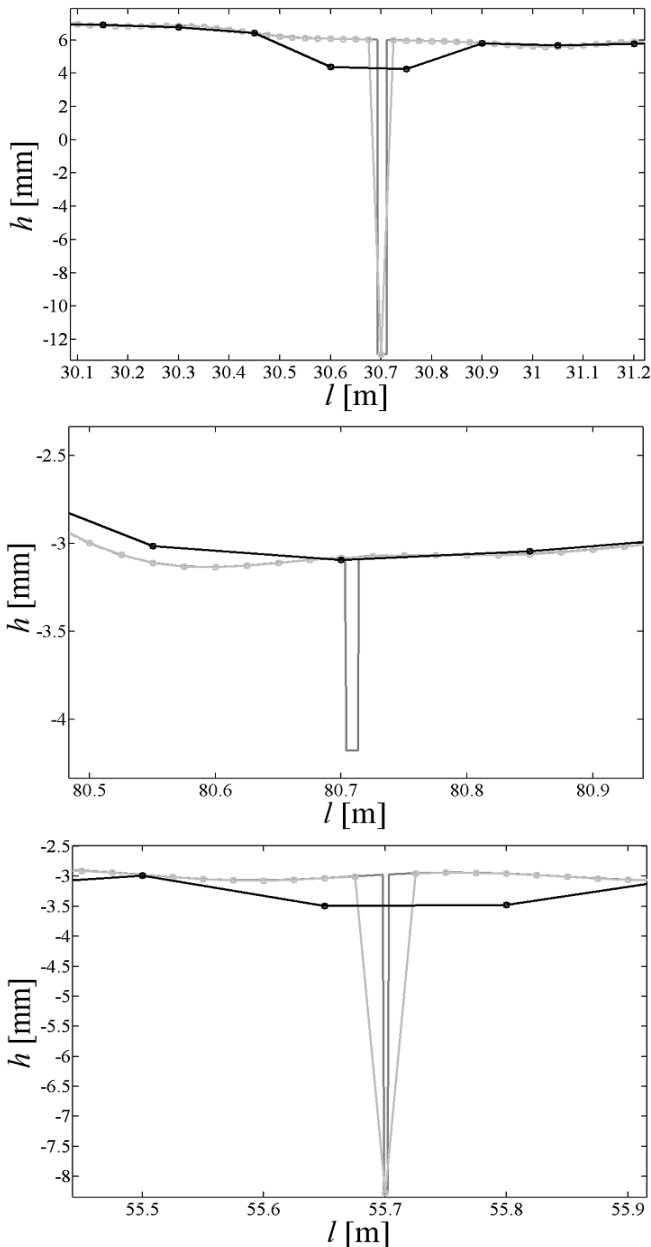


Fig. 6. Examples of the Resampling and Moving Average Influence on the Detection of Reflection Cracks (Dark Gray – Original Profile, Sampled at 1 mm; Light Gray – Resampled at 2.5 cm; Black – Moving Averaged by 30 cm and Resampled to $\Delta l = 15$ cm).

The variable Δ presents the mean percentage difference between the particular RUI calculated for the raw profile with distresses (RUI_{RD}) and for the pure random part of this profile (RUI_R) and is defined as follows:

$$\Delta (\%) = \frac{1}{N} \sum_{i=1}^N 100 \times \frac{RUI_{RD}(i) - RUI_R(i)}{RUI_R(i)} \quad (2)$$

where N is number of repetitions. The positive sign of variable Δ indicates that the mean value of the particular RUI calculated for the distressed profile is higher than value obtained for the pure random profile. The analysis of variance (function *anova1* in Matlab) was applied to the calculated RUI data to detect if the particular RUIs obtained for the distressed and random profile have the same mean.

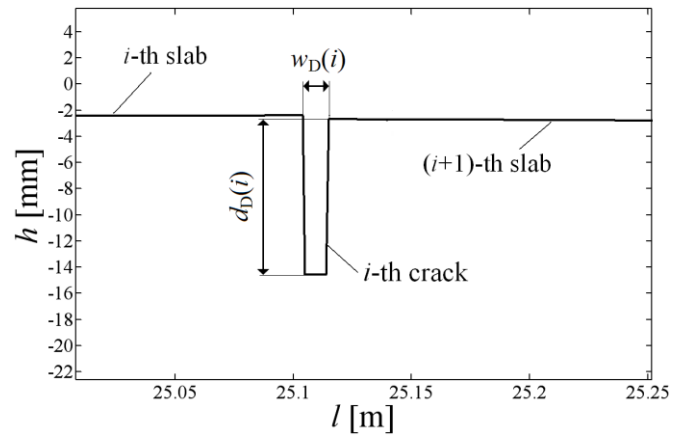


Fig. 7. The Main Dimension of the Simulated Reflection Cracks.

The statistical significance, p , is given in all Tables. The low value of p ($p < 0.05$) corresponds to the statistically significant differences between RUI_R and RUI_{RD} mean values. All computations were provided in Matlab®.

The influence of crack depth, crack width, crack distance, moving average and sampling interval on the simulation results will be assessed in further section.

The marked differences in estimated RUIs caused by distresses could be interpreted as follows:

- (a) The RUIs are able to reflect the presence of distresses in the road profile;
- (b) The RUIs have a limited sensitivity to reflect the current state of road profile, i.e. long wavelength contents, and their values are distorted by distresses. An impact of distresses on the RUIs will influence the longer-term rehabilitation decision making of composite pavements.

The small differences could be interpreted as follows:

- (a) The RUIs are not able to reflect the presence of the local distresses. Based on the crack dimensions, the vehicle fleet should be subjected to a repeated transient excitation. These short impulses decreased ride comfort and ride safety.
- (b) The RUIs are able to reflect the current state of road profile, i.e. long wavelength contents, and their values are not distorted by distresses.

Distresses of composite pavements are detected and picked up during pavement distress condition survey that provides defect details important for distress maintenance planning. Various roughness indexes are not normally meant for distress maintenance planning but for pavement rehabilitation consideration in Pavement Management System (PMS) as an overall serviceability condition of pavement sections. The question to ask is whether the distresses are an important factor affected roughness indexes that will influence the longer-term rehabilitation decision making.

Simulation Results

Table 2 presents the mean values for ten random road realizations. The following dimensions of the listed RUIs were used: C , C_L and C_S ($10^{-6} \text{ rad}^{-1} \text{ m}^{3-w}$), w , w_L , and w_S (—), RMS_H , RMS_L , RMS_M , and RMS_S (mm), IRI (mm/m); RN (—), PI (mm/m), PrI (in/mi), $\langle 2A_B \rangle$, $\langle 2A_F \rangle$, $\langle 2A_{RSE} \rangle$, and σ_{MCD} (mm), $RMSVA$ (mm/m^2). The crack

Table 2. Comparison of the Road Unevenness Indexes Calculated for the Pure Random Profiles and Profiles with Superimposed Reflection Cracks.

	Mean (RUI _R)	Mean (RUI _{RD})	Δ (%)	<i>p</i>	RANK
<i>C</i>	0.513	0.411	-19.9	0.001	4
<i>w</i>	2.533	2.143	-15.4	0	5
<i>C_L</i>	0.713	0.713	0	1	18
<i>C_S</i>	0.471	0.26	-44.6	0	2
<i>w_L</i>	2.352	2.351	-0.1	0.992	16
<i>w_S</i>	2.491	1.928	-22.6	0	3
RMS _H	2.992	2.995	0.1	0.99	16
RMS _L	4.038	4.038	0	1	18
RMS _M	0.869	0.871	0.3	0.946	15
RMS _S	0.329	0.514	56.3	0	1
IRI	1.289	1.306	1.3	0.608	14
RN	3.86	3.733	-3.3	0	10
PI	0.002	0.002	13	0	6
PrI	5.998	6.184	2.8	0.815	11
<2 <i>A_B</i> >	0.931	0.986	5.9	0.025	7
<2 <i>A_F</i> >	1.376	1.447	5.1	0.061	8
<2 <i>A_{RSE}</i> >	1.112	1.163	4.6	0.103	9
σ _{MCD}	0.871	0.885	1.6	0.601	12
RMSVA	0.774	0.786	1.6	0.594	12

depth and width were considered to be uniformly distributed random numbers in the intervals, $d_D = (0, 15)$ mm and $w_D = (5, 20)$ mm. The statistics of the generated cracks was as follows: $d_D = 7.41 \pm 4.39$ mm, and $w_D = 12.47 \pm 4.47$ mm. The standard competition ranking [44] was applied to the average absolute differences Δ . Ranking of RUIs is given in the last column of Table 2. The RUIs that are more sensitive to the distresses are ranked higher.

Eight of the nineteen unevenness indexes indicated the significant change ($p < 0.05$) in their means. Eleven RUIs indicated difference $< 5\%$. The spectrum parameters *C*, *w*, *C_S*, and *w_S*, further RMS_S, PI, and several straightedge indexes were most sensitive to the presence of cracks in profile. Only negligible difference was calculated for the RMS values and the spectrum parameters in medium- and long wave bands (RMS_H, RMS_M, RMS_L, *C_L*, *w_L*), and for IRI, RN and PrI too.

IRI, PI and RN were only slightly sensitive to the presence of cracks due to raw road data processing with a 25-cm moving average included in the IRI definition [30]. Further factor is the frequency response of the relative suspension velocity of the reference quarter-car model intended for the IRI or RN computation. This transfer function is most sensitive to the wavelength of ~ 2.1 m. PI is more sensitive to the presence of the cracks than IRI. PI is sensitive to shorter wavelengths than the IRI. The local peak of relative velocity transfer function of reference quarter-car model corresponds to the wavelength of ~ 0.67 m [32].

The insensitivity of the indicators characterized the long wavelength band seems to be logical. The mid-cord straightedge parameters (σ_{MCD}, RMSVA) are not able to detect the cracks presence. The limitation is in a clearance evaluation in the mid-cord and shift by half of the straightedge length.

The percentage differences in Table 2 for RN and PI are relatively small (-3.3% and 13%) but the analysis of variation indicates that the groups are significantly different ($p < 0.0001$). This was caused by small variability of data within the groups. For IRI, the small percentage difference was observed between the groups (1.3%) but *p*-value indicates that the mean values of the groups are the same ($p = 0.608$).

Influence of the Crack Depth

The simulated crack depth approximates the depth of reflection cracks that occurs in reality and the change of the sealant volume or damage of sealed cracks. The crack depth was considered to be uniformly distributed random number in the interval $(0, d_{D\text{MAX}})$ for $d_{D\text{MAX}} = 5, 10, 15,$ and 20 mm with statistics of particular groups for ten realizations: $d_D = 2.66 \pm 1.4$ mm, 4.84 ± 2.8 mm; 7.66 ± 4.15 mm, and 9.85 ± 5.75 mm. The crack width was considered to be uniformly distributed random number from $w_{D\text{MIN}} = 5$ mm to $w_{D\text{MAX}} = 20$ mm with statistics $w_D = 12.7 \pm 4.3$ mm. Table 3 presents the mean differences between results for the pure random profile and random profile with superimposed distresses (cracks) of variable depth. The standard competition ranking [44] was applied to the average absolute difference Δ . The ranking of RUIs is given in the last column of Table 3. A sum of absolute values of difference Δ for all four considered crack depths was used for ranking of RUIs in Table 3.

For the maximum depth, $d_{D\text{MAX}} = 5$ mm, RMS_S, *C*, *w*, and *w_S* show a significant difference between means of groups. For the maximum depth, $d_{D\text{MAX}} = 20$ mm, ten RUIs indicate a significant difference. Sixteen RUIs in Table 3 show differences $< 5\%$ for $d_{D\text{MAX}} = 5$ mm and eight RUIs for $d_{D\text{MAX}} = 20$ mm.

The marked changes in difference Δ were observed for RMS_S ($\sim 70\%$), *C_S* ($\sim 40\%$), *w_S* ($\sim 25\%$), *C* ($\sim 25\%$), *w* ($\sim 20\%$), and PI ($\sim 20\%$). The moderate changes were calculated for PrI ($\sim 9\%$), the straightedge indexes ($\sim 5\text{--}10\%$), and RN ($\sim 5\%$). IRI, *C_L*, *w_L*, RMS_H, RMS_L, RMS_M, σ_{MCD} or RMSVA were practically unchanged with an increase of the crack depth.

Influence of the Crack Width

The considered crack width was chosen to reflect the real width of reflective cracks. The crack width was considered to be uniformly distributed random number in the interval $(w_{D\text{MIN}}, w_{D\text{MAX}})$ as follows $(5, 10), (10, 15), (15, 20),$ and $(20, 25)$ mm with statistics of partial groups, $w_D = 7.51 \pm 1.55$ mm; 12.54 ± 1.46 mm; 17.55 ± 1.44 mm and 22.48 ± 1.44 mm. The crack depth was considered to be uniformly distributed number from $d_{D\text{MIN}} = 0$ to $d_{D\text{MAX}} = 15$ mm with statistics, $d_D = 7.57 \pm 4.34$ mm. The results are shown in Table 4. A sum of absolute values of difference Δ for all four considered crack widths was used for ranking of RUIs in Table 4.

Thirteen of the analyzed RUIs show a lower mean difference Δ than 5% for $w_{D\text{MAX}} = 10$ mm and nine for $w_{D\text{MAX}} = 25$ mm. The significant difference in the mean values was calculated for seven RUIs ($w_{D\text{MAX}} = 10$ mm) and ten RUIs ($w_{D\text{MAX}} = 25$ mm).

Most sensitive indicators to the increase of the crack maximum width from 10 mm to 25 mm were RMS_S ($\sim 60\%$), *C_S* ($\sim 20\%$), PI ($\sim 15\%$), *C*, *w_S*, and *w* ($\sim 10\%$). The moderate changes were

Table 3. The Influence of Crack Depth on the Road Unevenness Indexes Difference between Pure Random and Cracked Profiles.

d_{DMAX} (mm)	5		10		15		20		RANK
	Δ (%)	p							
C	-6.7	0.3436	-17.9	0.016	-26.6	0.0009	-30.8	0.0001	3
w	-3.4	0.0056	-9.6	0	-17.5	0	-21.7	0	5
C_L	0	1	-0.3	0.9641	-0.2	0.9884	0.9	0.9274	15
C_S	-13.4	0.0362	-32.5	0	-47.1	0	-53.6	0	2
w_L	0	1	0.1	0.9873	0	0.9937	-0.2	0.9622	18
w_S	-4.7	0.0001	-13.1	0	-23.5	0	-29	0	4
RMS_H	0	0.9955	0	0.9955	0.1	0.9865	0.5	0.9503	17
RMS_L	0	0.9994	0	0.9996	0	0.9973	0.1	0.9941	19
RMS_M	0	0.9946	-0.1	0.9838	0	0.992	0.6	0.8747	16
RMS_S	8.3	0.0001	25.3	0	56.9	0	80.8	0	1
IRI	0.1	0.9452	0.4	0.837	1.1	0.5355	2.3	0.2239	14
RN	-0.4	0.1562	-1.3	0.0013	-3.6	0	-5.3	0	11
PI	1.7	0.1566	5.1	0.0013	14.3	0	20.7	0	6
PrI	0.8	0.9725	0.2	0.9857	1	0.9978	9.9	0.6355	10
$\langle 2A_B \rangle$	0.9	0.5447	3.1	0.0537	7	0.0007	9.3	0	7
$\langle 2A_F \rangle$	0.9	0.6706	2	0.3819	5.6	0.0159	7.5	0.0066	8
$\langle 2A_{\text{RSE}} \rangle$	0.5	0.7099	1.5	0.3105	4.2	0.0068	6.9	0.0001	9
σ_{MCD}	0.1	0.976	0.1	0.988	2.2	0.5584	2.4	0.4998	12
RMSVA	0.1	0.9811	0	0.9973	2.2	0.5579	2.4	0.5022	13

Table 4. The Influence of the Crack Width on the Road Unevenness Indexes Difference between Pure Random and Cracked Profiles.

w_D (mm)	5–10		10–15		15–20		20–25		RANK
	Δ (%)	p							
C	-20	0.0003	-24.2	0.0001	-29.7	0	-29.2	0	3
w	-11.9	0	-15.5	0	-20.1	0	-21.8	0	5
C_L	0	1	0.5	0.9371	0	1	-0.1	0.9844	16
C_S	-35.6	0	-43.3	0	-51.6	0	-52.2	0	2
w_L	-0.1	0.9724	-0.2	0.9454	-0.1	0.9817	0.1	0.9816	18
w_S	-16.1	0	-20.9	0	-27.1	0	-28.9	0	4
RMS_H	0	0.9915	0.2	0.9659	0.2	0.9659	0.3	0.9403	15
RMS_L	0	0.9990	0	0.9959	0	0.9975	0	0.9968	19
RMS_M	0.1	0.9719	0.4	0.9175	0	0.9978	0.1	0.9848	16
RMS_S	33.7	0	51.8	0	76.2	0	91.7	0	1
IRI	0.5	0.8658	1.7	0.5431	1.5	0.6012	2.1	0.4567	14
RN	-1.9	0.0009	-3.2	0	-4.7	0	-5.9	0	11
PI	7.6	0.0009	12.6	0	18.5	0	23.7	0	6
PrI	4.6	0.9053	3.1	0.8544	7.1	0.7648	3.3	0.8424	10
$\langle 2A_B \rangle$	2.9	0.2129	5.5	0.013	8.8	0.0004	11.6	0.0003	7
$\langle 2A_F \rangle$	3.1	0.0922	4.3	0.0285	6.5	0.0033	9.4	0.0004	8
$\langle 2A_{\text{RSE}} \rangle$	2.9	0.1778	4.2	0.0418	6.4	0.0057	8.1	0.0058	9
σ_{MCD}	1.3	0.7046	2.7	0.4344	1.6	0.6592	1.3	0.7118	12
RMSVA	1.3	0.7041	2.7	0.4352	1.6	0.6559	1.3	0.7019	12

calculated for the straightedge indexes (~ 5 – 9%). The negligible changes ($< 5\%$) were observed for RN, IRI, C_L , w_L , RMS_H , RMS_L , RMS_M , σ_{MCD} or RMSVA.

Influence of the Crack Distance

Reflective cracks were considered to be placed in the profile at a constant distance l_D corresponding approximately to the slab length. Four different constant distances were considered, $l_D = 4, 6, 8,$ and 10 m. The crack width was assumed to be a function of the slab

length. Thus, the crack width was defined to be uniformly distributed random number in the interval, $w_D = (0.001l_D, 0.003l_D)$. The crack depth was considered to be uniformly distributed random number ranged from $d_{\text{DMIN}} = 0$ to $d_{\text{DMAX}} = 15$ mm. The statistics of the crack dimensions for all ten realizations was as follows, $d_D = 7.7 \pm 4.3$ mm and $w_D = 10.1 \pm 3.5$ mm, 15.3 ± 5.3 mm, 20.3 ± 7.3 mm, and 24.4 ± 9.0 mm, for particular distances. The results are shown in Table 5. A sum of absolute values of difference Δ for all four considered crack distances was used for ranking of RUIs in Table 5.

Table 5. The Influence of the Crack Distance on the Road Unevenness Indexes Difference between Pure Random and Distressed Profile.

l_D (m)	4		6		8		10		RANK
	Δ (%)	p							
C	-26.5	0	-28	0	-26.1	0	-29.1	0	3
w	-17.3	0	-18.4	0	-17.6	0	-20.7	0	5
C_L	0.3	0.9399	-0.6	0.8977	1	0.8238	0.1	0.9798	16
C_S	-47.1	0	-49	0	-46.9	0	-51.5	0	2
w_L	0	1	0.3	0.9536	-0.1	0.9795	0	0.9949	18
w_S	-23.5	0	-25	0	-23.7	0	-27.8	0	4
RMS_H	0.2	0.9786	0.1	0.984	0.2	0.9678	0.3	0.9626	15
RMS_L	0.1	0.9947	0	0.9993	0.3	0.9738	0	0.9986	17
RMS_M	0	0.9911	-0.2	0.9735	0.1	0.9719	0.3	0.9532	18
RMS_S	58.4	0	65.2	0	60.1	0	67.4	0	1
IRI	0.9	0.6537	1.4	0.4914	1.2	0.5596	2.3	0.2686	12
RN	-3.2	0.0003	-4	0	-3.8	0	-5.1	0	11
PI	12.7	0.0003	15.9	0	14.9	0	20.5	0	6
PrI	6	0.7654	1.7	0.907	12.9	0.5399	4.2	0.847	8
$\langle 2A_B \rangle$	7.1	0.0077	7.6	0.0096	7.3	0.0071	9.5	0.0028	7
$\langle 2A_F \rangle$	5.5	0.0002	5.7	0.0001	5.1	0.0015	7.9	0	9
$\langle 2A_{RSE} \rangle$	5.6	0.001	4.8	0.0103	4.5	0.0194	7.2	0.0007	10
σ_{MCD}	2.3	0.4664	0	0.9919	-0.4	0.9062	2.4	0.4451	13
RMSVA	2.3	0.4655	0	0.9909	-0.4	0.9035	2.4	0.4515	13

The change of the crack distance influenced only slightly the differences in RUIs. For ten RUIs, the significant change in mean values was observed for 4-m slab as well as for 10-m slab length. The percentage difference < 5 % was observed for 9 RUIs ($l_D = 4$ m), 11 RUIs (6 m), 10 RUIs (8 m), and 9 RUIs (10 m).

Influence of Moving Average and Sampling Interval

The computation of unevenness indexes defined in prEN 13036-5 standard proposal involves pre-processing of the profile, the output of which is a filtered and resampled (or pre-processed) profile. A sampling interval $\Delta l = 5$ cm is recommended. A moving average filter is commonly used tool in profile analysis to obtain a low-pass filtered profile [22]. The reason for data pre-processing by a moving average filter is to reflect the tire enveloping properties.

In the Federal Aviation Administration system, the 2.5 cm spaced samples are low-pass filtered by a moving average filter and sub-sampled to 15 cm [45]. The LTPP raw road profiles were originally sampled with an interval $\Delta l = 2.54$ cm and then were pre-processed with a 30.48-cm moving average and profiles were resampled to an interval of 15.24 cm.

Table 6 presents the influence of road data pre-processing on the RUIs. Two alternative moving average base lengths (B) and sampling intervals (Δl) were analyzed:

- (a) road data without pre-processing – $B = 0$ cm, $\Delta l = 2.5$ cm;
- (b) road data with pre-processing – $B = 30$ cm, $\Delta l = 15$ cm. A 30-cm moving average [46] was applied to the raw profiles as well as to the random parts and profiles were resampled to an interval of 15 cm.

The crack depth was considered to be uniformly distributed random number ranged from $d_{DMIN} = 0$ mm to $d_{DMAX} = 15$ mm and the crack width in the interval $w_D = 5$ –20 mm. The statistics of the crack dimensions was as follows: $d_D = 7.2 \pm 4.3$ mm and $w_D = 12.3$

± 4.4 mm.

For most of RUIs, the similar mean percentage differences between raw and random profiles were calculated, which were only slightly affected by data pre-processing. The greatest impact was observed for RMS_S , PI, or C_S indexes. The differences were changed due to data pre-processing by 10–40 %. These indexes are more sensitive to the short wavelength contents of the profile, which was suppressed by a moving average filtration applied to raw profile. The PSD measures C , w , or C_S slightly decreased for pre-processed data by ~ 5–10 %.

The mean differences for all five straightedge indexes were the same. The standards for the straightedge indexes estimation [45] use the processing of the raw road data with a 30-cm moving average and resampling to an interval of 15 cm.

Verification of Results on Real Test Section

The obtained results for simulated profiles were compared with results for real PCC test section #180606 with AC overlay. Section #180606 presents a road profile with maximum preparation of original JPCP section prior to AC overlay [47]. The most common features presented in this profile are the transverse and longitudinal reflection cracks [48]. Fig. 8 shows nine measurements of the left track of the road test section #180606 from years 1998 to 2005. Fig. 8 shows the increase of road roughness with time.

Median filter approach [49] was applied to a raw profile to identify a pure random part. It follows from the definition of the median filter that for the complete filtering of the non-random component including m discrete data, the $n \geq 2m + 1$ window length is needed. The window length for median filter was considered of order, $n = 16$ ($n\Delta l = 0.2$ m), which approximately corresponds to the double of the assumed maximum width of reflection cracks ($w_{DMAX} \sim 0.1$ m) in the processed road records.

Table 6. Influence of Road Data Pre-processing on Results for Simulated Road Profile.

#	RUI	without Pre-processing $B = 0$ cm, $\Delta l = 2.5$ cm				with Pre-processing $B = 30$ cm, $\Delta l = 15$ cm			
		Mean(RUI _R)	Mean(RUI _{RD})	Mean(Δ)	P	Mean(RUI _R)	Mean(RUI _{RD})	Mean(Δ)	p
1	C	0.632	0.520	-17.7	0	1.075	0.806	-25	0
2	w	2.608	2.282	-12.5	0	3.280	2.854	-13	0
3	C_L	0.694	0.694	0.1	1	0.695	0.698	0.4	0.9422
4	C_S	0.551	0.332	-39.7	0	1.683	0.856	-49	0
5	w_L	2.754	2.754	0	1	2.956	2.956	0	1
6	w_S	2.548	2.077	-18.5	0	3.484	2.880	-17.3	0
7	RMS _H	4.030	4.034	0.1	0.9641	3.466	3.470	0.1	0.9578
8	RMS _L	6.183	6.184	0	0.9958	6.183	6.184	0	0.9966
9	RMS _M	0.840	0.84	0.1	0.9744	0.852	0.853	0.1	0.9373
10	RMS _S	0.333	0.493	47.8	0	0.312	0.327	4.8	0
11	IRI	1.304	1.314	0.8	0.4986	1.241	1.250	0.7	0.5701
12	RN	3.855	3.743	-2.9	0	4.031	4.003	-0.7	0
13	PI	0.002	0.002	11.3	0	0.001	0.001	3.2	0
14	PrI	6.667	6.787	2.1	0.8811	6.368	6.630	6.5	0.7545
15	$\langle 2A_B \rangle$	0.955	0.995	4.2	0.0024	0.955	0.995	4.2	0.0024
16	$\langle 2A_F \rangle$	1.400	1.455	4	0.0124	1.4	1.455	4	0.0124
17	$\langle 2A_{RSE} \rangle$	1.135	1.174	3.4	0.0148	1.135	1.174	3.4	0.0148
18	σ_{MCD}	0.886	0.901	1.7	0.1962	0.886	0.901	1.7	0.1962
19	RMSVA	0.787	0.801	1.7	0.1986	0.787	0.801	1.7	0.1986

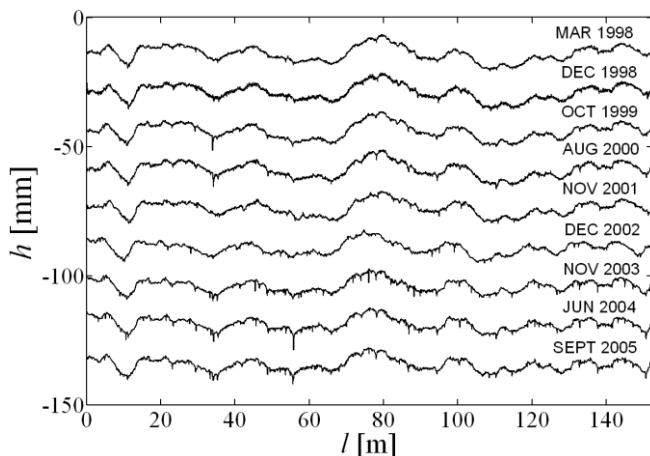


Fig. 8. Road Elevation of Right Track of Indiana Road Test Section #180606 Measured from Years 1998 to 2005 (Shifted by 20 mm).

In Table 7, a percentage difference of evaluated RUIs between raw profile and separated random part are presented for section #180606. The percentage difference Δ in Table 7 indicates a similar impact of the presence of cracks on the change of the road unevenness indicators as for the simulated profiles. A higher impact of distresses on the particular RUIs were observed for the spectrum parameters (C , w , C_S , and w_S), PI, RMS_S or the straightedge indexes.

Conclusions

The presented simulation study estimated the road distresses influence on the various roughness indexes. The results are applicable to composite pavements only.

From the results, following findings may be stated:

1. The proposed algorithm allows to control the different distress dimensions and to quantify the sensitivity of the various road unevenness indexes to the distress presence in a profile. The sensitivity is not affected by the change of the random part of profile.
2. Approximately half of nineteen analyzed road unevenness indicators were sensitive to the reflection cracks presence in the random profile. The remaining indicators show only negligible and statistically insignificant changes.
3. The most sensitive indicators to the cracks presence were detected to be the road elevation RMS value in the short wave band, the road elevation spectrum parameters in the whole and short wave bands and PI.
4. The negligible changes ($< 5\%$) were observed for the IRI, RN, PrI, or road elevation RMS values in the long and medium wave bands.
5. The most sensitive indicators to the increase of the crack maximum depth from 5 mm to 20 mm were RMS_S (percentage change $\sim 70\%$), C_S ($\sim 40\%$), w_S ($\sim 25\%$), C ($\sim 25\%$), w ($\sim 20\%$), and PI ($\sim 20\%$). The most sensitive indicators to the increase of the crack maximum width from 10 mm to 25 mm were RMS_S ($\sim 60\%$), C_S ($\sim 20\%$), PI ($\sim 15\%$), C , w_S , and w ($\sim 10\%$).
6. The change of the crack distance influenced only slightly the RUIs differences between random and distressed profiles.
7. The most sensitive indicators to the elevation data pre-processing were RMS_S ($\sim 45\%$), C , C_S and PI ($\sim 10\%$). A weak sensitivity was observed for the spectrum parameters and RMS values in the long and medium wave bands, IRI, RN or PrI.
8. The similar impact of the crack presence in the profile on the RUIs values as for the simulated profiles was identified for the measured profile.

Table 7. Percentage Difference Δ (Eq. (2)) for Measured Test Section #180606 (Left Track).

RUI	MAR 1998	DEC 1998	OCT 1999	AUG 2000	NOV 2001	DEC 2002	NOV 2003	JUN 2004	SEPT 2005	MEAN
C	-14	-13	-11	-11	-13	-11	-12	-11	-11	-11.9
w	-11	-13	-10	-11	-11	-12	-14	-14	-12	-12
C_L	0	0	0	0	2	0	0	0	0	0.2
C_S	-27	-33	-25	-31	-30	-32	-37	-33	-29	-30.8
w_L	0	0	0	0	0	0	0	0	0	0
w_S	-18	-22	-15	-18	-18	-18	-21	-20	-17	-18.6
RMS_H	0	0	0	0	0	0	0	0	0	0
RMS_L	0	0	0	0	0	2	1	2	2	0.8
RMS_M	4	1	2	2	1	1	1	2	3	1.9
RMS_S	28	45	22	25	21	16	25	18	20	24.4
IRI	1	1	1	2	1	1	2	3	2	1.6
RN	-3	-3	-2	-3	-2	-1	-3	-3	-3	-2.6
PI	12	15	10	11	10	7	12	11	11	11
PrI	3	-6	1	4	9	1	3	-1	3	1.9
$\langle 2A_B \rangle$	4	9	8	8	5	9	11	13	9	8.4
$\langle 2A_F \rangle$	4	7	4	5	5	1	6	7	5	4.9
$\langle 2A_{RSE} \rangle$	4	5	4	5	3	2	5	5	4	4.1
σ_{MCD}	2	1	1	2	2	2	0	1	1	1.3
RMSVA	2	1	1	2	2	2	1	1	1	1.4

Acknowledgments

This work has been undertaken within the grant No. 2/0058/13 of the VEGA Grant Agency of Slovak Academy of Sciences. The help of the LTPP InfoPave Support Team is highly appreciated.

Notation

$2A$ double amplitude (straightedge parameter) (mm)
 $\langle 2A \rangle$ mean value of the double amplitude (mm)
 $2A_B$ the maximum deviation between straightedge supports (mm)
 $2A_F$ the maximum deviation over full straightedge length (mm)
 $2A_{RSE}$ the maximum deviation of the interior profile points from the straight line (mm)
 B base length (m)
 B_e frequency resolution (rad/m)
 C unevenness index ($10^{-6} \text{ rad}^{w-1} \text{ m}^{3-w}$)
 C_L, C_S unevenness index for long and short wave bands respectively ($10^{-6} \text{ rad}^{w-1} \text{ m}^{3-w}$)
 DOT Department of Transportation
 h road profile elevation (i.e., vertical road displacement) (m)
 h_D pure distress profile (m)
 h_R pure random profile (m)
 h_{RD} random profile with superimposed distresses (m)
 d_D crack depth (mm)
 $G_H(\Omega)$ one-sided road elevation power spectral density (m^3/rad)
 IRI International Roughness Index (mm/m)
 l length (m)
 l_D distance of successive cracks (m)
 L wavelength (m)
 L_{tot} total length of section (m)
 LTPP Long Term Pavement Performance
 MCD the mid-cord deviation between the road profile and the

rolling straightedge (mm)
 N_D number of reflection cracks per section
 N number of repetitions
 p significance
 PCC Portland cement concrete
 PI Profile Index (mm/m)
 PrI Profilograph Index (mm/km)
 PMS Pavement Management System
 PSD power spectral density
 RMSVA root mean square vertical acceleration (mm/m^2)
 RMS_H root mean square value of the longitudinal road profile elevations (mm)
 RMS_L, RMS_M, RMS_S root mean square values of the longitudinal road profile elevations in the long, medium, and short wave bands (mm)
 RN Ride Number (-)
 RUI road unevenness indicator
 RUI_R road unevenness indicator for the pure random profile
 RUI_{RD} road unevenness indicator for the random profile with superimposed cracks
 SE straightedge
 SPS Specific Pavement Study
 VA vertical acceleration (mm/m^2)
 w_D crack width (mm)
 w waviness (-)
 w_L, w_S waviness for long and short wave bands respectively (-)
 Λ straightedge length (m)
 σ_{MCD} standard deviation of the mid-cord deviation (mm)
 Δ percentage difference between the road unevenness indexes calculated for the pure random profile and combined profile with superimposed cracks (%)
 Δl sampling interval (m)
 Ω angular spatial frequency (rad/m)

References

1. Highway Statistics 2012 [online]. (2013). Federal Highway Administration, Washington DC, Available from: <http://www.fhwa.dot.gov/policyinformation/statistics/2012/> [Accessed 15 April 2014].
2. Flintsch, G.W., Diefenderfer, B.K., and Nunez, O. (2008). Composite Pavement Systems: Synthesis of Design and Construction Practices, Report No. *FHWA/VTRC 09-CR2*, Virginia Tech Transportation Institute, Blacksburg, VA, USA, 60 p.
3. Hein, D.K., Olidis, C., Magni, E., and MacRae, D. (2002). A method for the investigation and validation of composite pavement performance including the use of the falling weight deflectometer, Pavement Evaluation 2002 - A Joint Conference of the FWD and Road Profilers User Groups, Roanoke, VA, USA.
4. Kováč, M., Remišová, E., Čelko J., Decký, M., and Ďurčanská, D. (2012). *Diagnostic of parameters of roads operational capability*, EDIS – Printing House of the University of Žilina, Žilina, Slovakia, ISBN 978-80-554-0568-1 (in Slovak).
5. Bennert, T. (2010). Flexible Overlays for Rigid Pavements, Report No. *FHWA-NJ-2009-014*, New Jersey Department of Transportation, Trenton, NJ, USA, 159 p.
6. Miller, J.S. and Bellinger, W.Y. (2003). Distress Identification Manual for the Long-Term Pavement Performance Program (Fourth Revised Edition), Report No. *FHWA-RD-03-031*, Federal Highway Administration, McLean, VA, USA.
7. McGhee, K.H. (1995). Design, construction, and maintenance of PCC pavement joints, NCHRP Synthesis of Highway Practice, Vol. 211, Transportation Research Board, Washington, DC, USA.
8. Byrum, C.R. (2000). Analysis by high-speed profile of jointed concrete pavement slab curvatures, *Transportation Research Record*, No. 1730, pp. 1–9.
9. Wen, H. and Chen, C. (2007). Factors Affecting Initial Roughness of Concrete Pavement, *Journal of Performance and Constructed Facilities*, 21(6), pp. 459–464.
10. Khazanovich, L., Darter, M.I., Bartlett, R.J., and McPeak, T. (1998). Common characteristics of good and poorly performing pavements. Report No. *FHWA-RD-97-131*, Federal Highway Administration, U.S. Department of Transportation, Washington, DC, USA.
11. Perera, R.W. and Kohn, S.D. (2002). Issues in pavement smoothness: a summary report, NCHRP Web Document 42, National Research Council, Washington, DC, USA.
12. Selezneva, O., Jiang, J., and Tayabji, S.D. (2000). Preliminary evaluation and analysis of LTPP faulting data, Report No. *FHWA-RD-00-076*, Federal Highway Administration, U.S. Department of Transportation, Washington, DC, USA.
13. Byrum, C.R. and Perera, R.W. (2005). The effect of faulting on IRI values for jointed concrete pavements, *Proceedings of 8th International Conference on Concrete Pavements: Innovations for Concrete Pavement: Technology Transfer for the Next Generation*, American Association State Highway and Transportation Officials (AASHTO), Vol. 2, 755–770.
14. Liu, C. and Wang, Z. (2008). Influence of joints on ride quality and roughness index, *Road Materials and Pavement Design*, 9(1), pp. 111–121.
15. Morian, D.A., Gibson, S.D., and Epps, J.A. (1998). Concrete pavement maintenance treatment performance review: SPS-4 5-year data analysis. Report No. *FHWA-RD-97-155*, Federal Highway Administration, U.S. Department of Transportation, Washington, DC, USA.
16. Hall, K.T. and Crovetto, J.A. (2000). LTPP data analysis: relative performance of jointed plain concrete pavement with sealed and unsealed joints, NCHRP Web Document 32, National Cooperative Highway Research Program, Transportation Research Board, Washington, DC, USA.
17. Smoothness Specifications Online [online]. (2012). The Transtec Group, Austin, Texas, USA, Available from: <http://www.smoothpavements.com> [Accessed 20 January 2014].
18. Willet, M., Magnusson, G., and Ferne, B.W. (2000). FILTER experiment – Theoretical study of indices, *FEHRL Tech. Note 2000/02*, Transport Research Laboratory, Crowthorne, Berkshire, UK.
19. Boscaino, G. and Praticò, F.G. (2001). A classification of surface texture indices of pavement surfaces, *Bulletin des Laboratoires des Ponts et Chaussées*, Vol. 234, pp. 17–34.
20. Delanne, Y. and Pereira, P.A.A. (2001). Advantages and limits of different road roughness profile signal-processing procedures applied in Europe, *Transportation Research Record*, No. 1764, pp. 254–259.
21. Praticò, F. (2004). Nonstrictly-ergodic signals in road roughness analyses: A theoretical and experimental study, *Proceedings of 2nd International Congress Societa Italiana Infrastrutture Viarie (SIIV): New Technologies and Modeling Tools for Roads—Application to design and management*, University of Florence, Florence, Italy.
22. Sayers, M.W. and Karamihas, S.M. (1998). The little book of profiling, University of Michigan, MI, USA.
23. Wilde, W.J. (2007). Implementation of an International Roughness Index for Mn/DOT Pavement Construction and Rehabilitation, *Report MN/RC-2007-09*, Research Services Section, Minnesota Department of Transportation, St. Paul, USA, 133 p.
24. Chemistruck, H.M., Detweiler, Z.R., Ferris, J.B., Reid, A.A., and Gorsich, D.J. (2009). Review of current developments in terrain characterization and modelling, *Proceedings of SPIE—The International Society for Optical Engineering*, The International Society for Optical Engineering, Bellingham, WA, USA.
25. European Committee for Standardization (CEN) (2014). prEN 13036-5: 2014. Road and airfield surface characteristics – Test methods. Part 5: Determination of longitudinal unevenness indices. European Committee for Standardization, Brussels, Belgium.
26. Andrén, P. (2006). Power spectral density approximations of longitudinal road profiles, *International Journal of Vehicle Design*, 40(1/2/3), pp. 2–14.

27. ISO (1995). ISO 8608: 1995. Mechanical vibration—Road surface profiles—Reporting of measured data. International Standardization Organization, Geneva, Switzerland.
28. Kropáč, O. and Múčka, P. (2008). Indicators of longitudinal unevenness of roads in the USA, *International Journal of Vehicle Design*, 46(4), pp. 393–415.
29. Múčka, P. (2012). Longitudinal road profile spectrum approximation by split straight lines, *Journal of Transportation Engineering–ASCE*, 138(2), pp. 243–251.
30. Sayers, M.W. (1995). On the calculation of IRI from longitudinal road profile, Paper No. 950842, Transport Research Board, Washington, DC, 24 pp.
31. ASTM (2003). E1926-98: 2003. Standard practice for computing International Roughness Index of roads from longitudinal profile measurements, American Society for Testing and Materials, West Conshohocken, PA, USA.
32. Sayers, M.W. and Karamihas, S.M. (1996). Interpretation of road roughness profile data, *Report UMTRI-96-101*, University of Michigan, Transportation Research Institute, MI, USA.
33. Song, I. and Teubert, C.H. (2007). Current California profilograph simulations and comparisons, *Proceedings of 2007 FAA Worldwide Airport Technology Transfer Conference*, Federal Aviation Administration, FAA Airport Technology R&D Branch, Atlantic City, NJ, USA.
34. Shon, S., Yoo, I., Lee, S., and Kim, J. (2008). Implementation and Verification of a New California Type Profilograph Based on WLAN, *Proceedings from the 25th International Symposium on Automation and Robotics in Construction - ISARC-2008*, Vilnius, Lithuania: Vilnius Gediminas Technical University Publishing House 'Technika', pp. 384–390.
35. ASTM (2008). E1274-03: 2008. Standard Test Method for Measuring Pavement Roughness Using a Profilograph, American Society for Testing and Materials, West Conshohocken, PA, USA.
36. Farias, M.M. and Souza, R.O. (2009). Correlations and analyses of longitudinal roughness indices, *Road Materials and Pavement Design*, 10(2), pp. 399–415.
37. Tsai, C.-Y., Chou C.-P., and Chen. A.-C. (2012). The study of the relationship between IRI and 3m straightedge acceptance specification, *Journal of the Chinese Institute of Engineers*, 35(4), pp. 439–448.
38. Perera, R.W., Byrum, C., and Kohn, S.D. (1998). Investigation of development of pavement roughness, Report No. *FHWA-RD-97-147*, Federal Highway Administration, U.S. Department of Transportation, Washington, DC, USA.
39. Chang, G., Nazef, A., Watkins, J., and Karamihas, S. (2010). Automated Fault Measurement (AFM) in ProVAL, *Proceedings of Pavement Engineering 2010*, Virginia Tech Transportation Institute, 25–27th October 2010, Roanoke, VA, USA.
40. Chang, G., Watkins, J., and Orthmeyer, B. (2011). Practical Implementation of Automated Fault Measurement Based on Pavement Profiles, International Symposium on Pavement Performance Trends, Advances, and Challenges, American Society for Testing and Materials, Tampa, Florida, USA.
41. Byrum, C.R. (2010). Evaluating effectiveness of dowels in jointed-concrete pavements with faulting data from rapid-travel profilers, *Transportation Research Record*, No. 2154, pp. 32–43.
42. Múčka, P. (2012). Relationship between International Roughness Index and straightedge index, *Journal of Transportation Engineering–ASCE*, 138(9), pp. 1099–1112.
43. Múčka, P. and Kropáč, O. (2009). Properties of random component of longitudinal road profile influenced by local obstacles, *International Journal of Vehicle Systems Modelling and Testing*, 4(4), pp. 256–276.
44. Pozzi, F. (2008). Rankings [Computer software]. Available from: <http://www.mathworks.com/matlabcentral/fileexchange/19496-rankings> [Accessed 14 April 2008].
45. Song, I. and Hayhoe, G.F. (2006). Airport pavement roughness index relationships using the Federal Aviation Administration (FAA) profiling system, *Proceedings of 2006 Airfield and Highway Pavement Specialty Conference*, ASCE, Reston, VA, USA, pp. 741–752.
46. Aguilera, C.A.V. (2008). Moving_average v3.1 [Computer software]. Available from: <http://www.mathworks.com/matlabcentral/fileexchange/12276> [Accessed 8 July 2009].
47. Ambroz, J.K. and Darter, M.I. (2005). Rehabilitation of jointed Portland cement concrete pavements: SPS-6 – Initial evaluation and analysis. Report No. *FHWA-RD-01-169*, Federal Highway Administration, McLean, VA, USA.
48. LTPP InfoPave [online]. (2014). Federal Highway Administration, US Department of Transportation, Available from: www.infopave.com [Accessed 20 February 2014].
49. Kropáč, O. and Múčka, P. (2011). Specification of obstacles in the longitudinal road profile by median filtering, *Journal of Transportation Engineering–ASCE*, 137(3), pp. 214–226.